INTERANNUAL CHANGES IN GLOBAL SURFACE DUST COVERAGE USING MARS CLIMATE SOUNDER. J. Bapst[1] and S. Piqueux[1], [1]Jet Propulsion Laboratory, California Institute of Technology, Pasadena, CA 91109, USA, jonathan.bapst@jpl.nasa.gov

Introduction: The current climate of Mars is punctuated by annually-recurring regional-scale and intermittently-occurring (every 3–5 Mars Years) global-scale dust storms where dust is lifted and transported via atmospheric circulation. In the atmosphere, dust absorbs short-wavelength solar radiation, reducing the amount of sunlight reaching the surface, and increasing downwelling long wavelength radiation [1]. On the surface, dust influences the albedo and thermal properties, hence the energy absorbed, by brightening soils, darkening ices, and insulating the surface regolith due to its very low thermal inertia [2].

Interannual changes in surface dust coverage are expected based on the analysis of spacecraft observations [2–4], and theoretical climate models [5,6]. However, the amount, rate, and spatial variability concerning this redistribution of dust is not well understood and is the motivation for this work. Here, we use infrared observations acquired from orbit to constrain changes in dust coverage and/or thickness from one Mars year to the next. Results have implications for the global transport of dust and the climate of Amazonian Mars.

Methodology: Thermal emission measured by the Mars Climate Sounder (MCS) infrared radiometer aboard Mars Reconnaissance Orbiter allows accurate derivation of surface and atmospheric temperature. Derived surface temperature can be used in concert with thermal diffusion models (here, we employ KRC [7]), to constrain the homogeneous thermal inertia, which is an important quantity for interpreting the geological material(s) comprising the surface and near-subsurface. We simultaneously fit both thermal inertia and thermometric (i.e., modeled) albedo using MCS-derived nighttime and daytime temperatures. Daytime surface temperatures are strongly influenced by albedo while nighttime temperatures are controlled primarily by thermal inertia [8].

We analyzed 7 Mars years (Mars Year 28–34) of daytime and nighttime retrieved surface temperatures from MCS (e.g., Figure 1). We further divide annual data into 30° L_S windows, but maintain ample global coverage at 1°×1° latitude by longitude spatial resolution. Interannual changes in thermometric albedo and thermal inertia are assessed at the same seasonal window between Mars years to minimize the influence of known seasonal cycles in atmospheric processes (e.g., water ice clouds and dust storms; [9,10]). Seasonal changes in atmospheric dust are accounted for by including climatology information after [10] in our thermal model. Additionally, derived properties are assessed regionally, instead of at the 1°×1° resolution level (i.e., individual bins are not compared to one another; see Figure 2). Derived albedo and thermal inertia are both displayed as the mean value within the region sampled where error bars indicate the standard deviation. Year-to-year changes in these properties are interpreted in the context of changing dust thickness and location.

To test for interannual changes in dust coverage we focus on specific regions through time. Here we show preliminary results for five different regions. These include areas of relatively low-dust index (Syrtis Major and Chryse Planitia; [11]), rover landing sites (Gale Crater and Meridiani Planum), and a region where climate models suggest the most extreme fluxes in surface dust (Hellas Basin; [5]). Note, our regions sample an area of 20°×20°, except for those over rover landing sites where we sample areas of 10°×10°. We have not included results over the dust-rich regions of the surface but will present those derivations at the time of the conference. Our results cover four times of year: L_S=0–30°, L_S=90–120°, L_S=180–210°, and L_S=270–300° and data are plotted at each seasonal window midpoint.

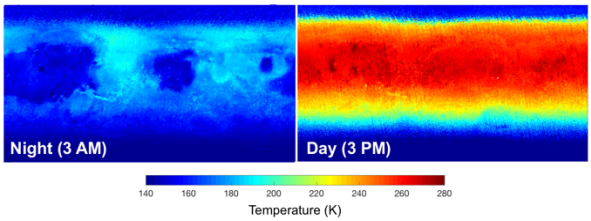

Figure 1. Example global MCS temperatures from MY30, L_S=30–60°, and binned at 1°×1° latitude/longitude. Daytime and nighttime temperature pairs, in conjunction with a thermal diffusion model (KRC), are used to derive a best-fit thermal inertia and best-fit surface albedo. Note, in this figure temperatures are partially interpolated for display purposes (interpolated data are not analyzed).

Results: Derived values (i.e., best fit) of albedo and thermal inertia are shown in reference to their location on a global map of Mars (Figure 2). Values for thermal inertia are in units of J m^{-2} K^{-1} $s^{-1/2}$. The global map includes the measured dust-index (a proxy for dust coverage; [11]) overlaid on a grayscale shaded-relief map.

For all the regions, both albedo and thermal inertia show cyclical behavior on an annual period, with some

regions more pronounced than others. In general, the data show consistent values year-to-year across the ~7 Mars Years analyzed. Gale Crater, and to some extent Merdiani Planum, show a notable dearth in values beyond Mars Year 30 due to the operation and relay priorities of surface assets (i.e., fewer MCS observations).

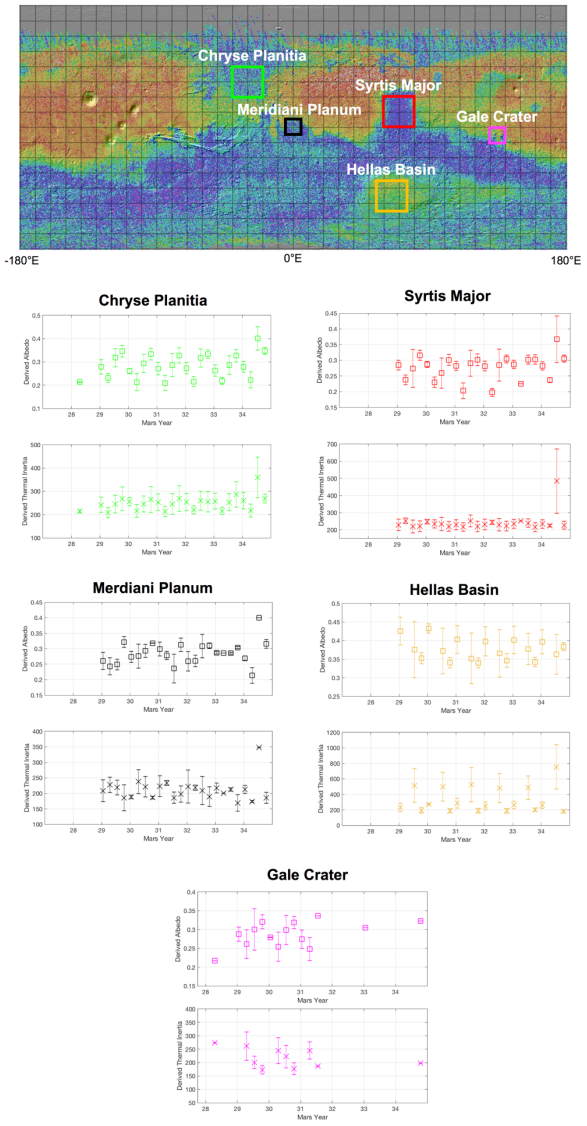

Figure 2. Five regional examples of derived albedo and thermal inertia over 7 Mars Years. The outline color of each region corresponds to data in the plots below. Note the changing vertical axis and the cyclical behavior indicating the seasonal influence on thermally-derived properties. Global map shows dust index (Ruff2002) overlaid on a shaded relief background; redder values indicate higher dust index.

Discussion: Evidence for change in dust coverage is expected as a secular, interannual shift in derived albedo and/or derived thermal inertia. The derived properties discussed here, although exhibiting significant intra-annual variation, show little evidence for change that would be interpreted as change in dust coverage. Aspects of the data will be discussed in more detail below.

Intra-annual Trends: The intra-annaul, cyclical behavior in derived values is suggestive of seasonal processes having influence on measured temperatures that is not entirely accounted for in our thermal model (e.g., water-ice clouds, subsurface layering). The largest fluctuations are observed in our mid-to-high latitude examples (i.e., Chryse Planitia and Hellas Basin), consistent with influence from subsurface ice and/or seasonal ices at the surface and aerosols in the atmosphere. Derived albedo values are systematically higher (~0.1) than those measured by TES (Thermal Emission Spectrometer; [12]). Values of derived thermal inertia, and their seasonal variation, are consistent with published values [13].

Meridiani Planum: Derived properties in Meridiani do not exhibit as clear a seasonal pattern as other regions. In Mars Years 29–31, there is evidence for a secular increase in derived albedo for L_S=0–30° and L_S=90–120°. This coincides with increased thermal inertia and so contradicts an increase in dust coverage.

Mars Year 34: Derived properties in Mars Year 34, at L_S=180–210°, show extreme variability compared to data from other Mars Years for most regions. This is explained by the onset of the planet-encircling dust event that began and grew to a global event during this timeframe [14], thus affecting the accuracy of MCS surface retrievals. Data from L_S=270–300° support a return to pre-storm behavior seen in prior years.

Acknowledgement: Part of this work was performed at the Jet Propulsion Laboratory, under a contract with NASA. US Government support acknowledged.

References: [1] Smith, M. (2004) *Icarus*, **167**, 148–165 [2] Szwast, M. A. et al. (2006) *J. Geophys. Res.,* **111**, E11008 [3] Cantor, B. A. (2007) *Icarus,* **186**, 60–96 [4] Vincendon, M (2008) *Icarus,* **196**, 488–505 [5] Basu, S. and Richardson, M. I. (2004) *J. Geophys. Res. E Planets,* **109**, 1–25 [6] Kahre, M. A. et al. (2006) *J. Geophys. Res.* **111,** E06008 [7] Kieffer H. H (2013) *JGR Planets* **118**, 451–470 [8] Mellon, M. T. et al. (2000) *Icarus* **148,** 437–455 [9] Smith, M. D. (2008) *Annu. Rev. Earth Planet. Sci.* **36,** 191–219 [10] Montabone, L. *et al.* (2015) *Icarus* **251,** 65–95 [11] Ruff, S. W. and Christensen, P. R. (2002) *J. Geophys. Res. E Planets* **107,** 10–1 [12] Christensen, P. R. *et al.* (2001) *J. Geophys. Res. Planets* **106,** 23823–23871 [13] Putzig, N. E. and Mellon, M. T. (2007) *Icarus* **191,** 68–94 [14] Kass, D. M. et al. (2019) *Geophysical Research Letters*, **46**